STATISTICS, OPTIMIZATION AND INFORMATION COMPUTING
Stat., Optim. Inf. Comput., Vol. **x**, Month 2024, pp 0–13.
Published online in International Academic Press (www.IAPress.org)

Advanced Sech-Tanh Optimization Algorithm for the Optimal Sizing and Placement of PV Systems and D-STATCOMs in Distribution Networks

Oscar Danilo Montoya [1,*], Edwin Rivas-Trujillo [1], Luis Fernando Grisales-Noreña [2]

[1] *Facultad de Ingeniería, Universidad Distrital Francisco José de Caldas, Bogotá D.C. 110121, Colombia*
[2] *Grupo de Investigación en Alta Tensión-GRALTA, Universidad del Valle, Cali 760015, Colombia.*

Abstract This paper presents an innovative approach that employs the Sech-Tanh optimization algorithm (STOA) for the simultaneous integration of photovoltaic (PV) systems and distribution static compensators (D-STATCOMs) into distribution networks. Our proposal uses a discrete-continuous encoding scheme to determine the optimal location (nodes) and size (capacities) of these devices. A power flow analysis based on the successive approximations method is implemented to solve the power flow equations, evaluating technical parameters such as voltage profile and power injection. The problem is addressed through a master-slave optimization strategy, wherein the STOA is integrated with the power flow approach to obtain optimal solutions. The performance of this methodology is validated using 33- and 69-bus systems, showing notable improvements over traditional optimization techniques like the vortex search algorithm (VSA) and the sine-cosine algorithm (SCA). The results highlight reductions of approximately 35.5480% and 35.6801% in the objective function when applying the STOA in both test systems. Furthermore, the STOA reports reduced computational efforts in comparison with the VSA and the SCA, confirming its effectiveness. All numerical analyses are conducted using MATLAB 2024a.

Keywords Sech-Tanh Optimization Algorithm (STOA); Photovoltaic System (PV); Distribution Static Compensator (D-STATCOM); Power Flow Analysis; Distribution Network Optimization.

AMS 2010 subject classifications 62J07

DOI:10.19139/soic-2310-5070-2164

1. Introduction

1.1. General context

In recent years, the issue of energy efficiency in electrical networks has sparked considerable attention due to the increasing demand for reliable and sustainable energy. As power systems evolve, the need for more efficient electricity distribution has become critical in the struggle to reduce losses and improve the stability of electrical grids [1]. Optimizing distribution networks, where most energy losses occur, is a crucial step towards achieving higher energy efficiency [2]. This optimization not only ensures the delivery of electricity with minimal waste but also helps to meet growing energy demands, especially in densely populated areas [3]. The integration of renewable energy sources, particularly photovoltaic systems (PVs), has emerged as an effective solution to enhance the efficiency of electrical networks while contributing to sustainability goals [4].

Including PV systems in distribution networks offers significant environmental advantages, as it helps to reduce greenhouse gas emissions [5]. These systems convert solar energy into electricity, thereby supporting the transition to cleaner energy sources [6]. Nevertheless, their efficiency can be further enhanced by combining them with

*Correspondence to: O. D. Montoya (Email: odmontoyag@udistrital.edu.co). Facultad de Ingeniería, Universidad Distrital Francisco José de Caldas, Bogotá D.C. 110121, Colombia.

ISSN 2310-5070 (online) ISSN 2311-004X (print)

reactive power compensators (*e.g.*, distribution static compensators, or D-STATCOMs) [7]. This combination of active (*i.e*, PVs) and reactive power compensation not only improves voltage regulation and power quality; it also minimizes power losses in the grid [8]. Therefore, the integration of both PVs and D-STATCOMs in distribution networks offers a promising solution for achieving optimal energy efficiency while mitigating the environmental impact of traditional power generation methods.

1.2. Motivation

The integration of PVs and D-STATCOMs in distribution networks has been extensively studied, given these devices' ability to improve energy efficiency and system reliability [8]. However, with the continuously growing electricity demand and the global push for renewable energy integration, further research is essential for enhancing the effectiveness of these technologies in distribution systems. The dynamic nature of power flows in grids with a high penetration of distributed generators (DGs), especially renewable sources like PVs, implies the need for optimization strategies that can effectively manage active and reactive power flows [9]. Although significant advancements have been made in incorporating active and reactive power compensators for voltage stability and losses minimization, there is still a gap when it comes to fully optimizing their location and size with the purpose of maximizing the overall system performance [7]. Therefore, continuous research is critical in order to better understand the synergies between PVs and D-STATCOMs, ensuring a reliable and efficient energy supply while meeting sustainability goals [10].

Furthermore, the development of new optimization techniques (*e.g.*, metaheuristic algorithms) plays a vital role in improving the operational efficiency of distribution networks [10]. Traditional optimization methods often struggle with the complex, nonlinear nature of power systems that incorporate renewable energy sources and compensators. To address these challenges, novel metaheuristic algorithms like the Sech-Tanh optimization algorithm (STOA) offer a promising solution [11]. These methods are capable of handling the high-dimensional and multi-modal search spaces that are typical of power distribution networks, providing better results in terms of speed and accuracy when compared to conventional techniques [7]. Hence, proposing and refining these advanced optimization methods is crucial for ensuring the effective integration of PVs and D-STATCOMs and enhancing the performance of modern electrical distribution systems [8].

1.3. Literature review

Recent studies have extensively explored the integration of PVs and D-STATCOMs in medium-voltage distribution networks, seeking optimization techniques for their siting and sizing. Several optimization methods have been proposed, including the vortex search algorithm (VSA), the generalized normal distribution algorithm (GNDO), and multi-verse optimization (MVO). For instance, the authors of [7] employed the VSA to minimize the net present value of investment and operating costs over a 20-year period. While effective, this approach lacked comparative analyses with other optimization techniques. In contrast, the work by [8] demonstrated the superiority of the GNDO by improving upon the results obtained with the VSA, while the authors [12] highlighted the effectiveness of MVO in achieving better performance than the VSA in optimizing PV and D-STATCOM deployment in 33- and 69-bus distribution networks.

Hybrid analytical and metaheuristic methods have also been explored to enhance the accuracy and robustness of optimization solutions. In [13], a hybrid approach combining particle swarm optimization (PSO) with analytical methods was proposed to optimize the siting and sizing of DGs and D-STATCOMs. This method also incorporated a probabilistic load model that used Monte Carlo simulations to address demand variability, yielding significant improvements regarding losses minimization and voltage stability in a real distribution network from South Kerman (Iran). Similarly, the authors of [14] introduced a method for integrating microgrids and D-STATCOMs to improve voltage profiles and reduce power losses. By employing PSO for sizing and utilizing voltage stability indices for placement, the approach demonstrated notable performance enhancements in an IEEE 30-bus system.

The potential of PV-STATCOM devices to enhance grid stability and power quality has also been extensively explored. In [15], a smart inverter-based PV-STATCOM system was developed, capable of providing continuous voltage control during both daytime and nighttime. This system temporarily suspended real power generation during disturbances to maximize reactive power support, exhibiting low-voltage ride-through capabilities and

rapid response times akin to conventional STATCOMs. Moreover, the authors of [16] introduced a PV-STATCOM approach to mitigate harmonics and zero-sequence components from unbalanced nonlinear loads, achieving significant reductions in total harmonic distortion (from 28.80% to 2.03%) and zero-sequence components (from 31.50% to 4.26%). These systems demonstrated adaptability to variations in solar radiation and load conditions, contributing to enhanced power quality and grid stability.

The reviewed works underscore three main aspects: advancements in optimization techniques for PV and D-STATCOM placement and sizing, the emergence of hybrid analytical-metaheuristic approaches to address complex system requirements, and the innovative applications of PV-STATCOM systems for improving grid stability, harmonics mitigation, and power quality. These contributions provide a robust foundation for further developments in the integration of distributed energy resources and reactive power compensation devices into modern power systems.

1.4. Contributions and scope

Based on the above-presented literature review, this research introduces a novel master-slave optimization framework for the simultaneous integration of PVs and D-STATCOMs in medium-voltage distribution networks. In the master stage, the STOA is employed as the primary solution method via a hybrid discrete-continuous encoding strategy. Here, discrete encoding specifies the optimal locations for the installation of PVs and D-STATCOMs, while continuous encoding determines their nominal capacities. The slave stage makes use of the successive approximations power flow method to validate the technical feasibility of the proposed solutions while ensuring compliance with voltage regulations and precise power injection into the distributed energy resources (DERs). The numerical results demonstrate the superiority of the STOA approach, providing enhanced solutions in comparison with those reported in the literature, including the VSA discussed in [7], and the sine-cosine algorithm (SCA).

The scope of this research encompasses several critical aspects, including the electrical characteristics of the studied distribution network, which were obtained from real measurements of daily active and reactive power demand profiles at the substation terminals, as provided by the corresponding utility. Additionally, a solar generation profile was elaborated by analyzing and processing historical solar resource data, which allowed determining the most probable solar generation curve for the region served by the medium-voltage feeder. For benchmarking purposes, the VSA, as described in [7], was implemented under identical parametric conditions to ensure a fair comparison.

1.5. Document structure

The structure of this document is as follows. Section 2 introduces the optimization model developed for optimally siting and sizing of PVs and D-STATCOMs in distribution networks. This model employs a mixed-integer nonlinear programming (MINLP) approach to minimize the total investment and operating costs over a 20-year planning horizon. Section 3 explains the proposed solution methodology, which integrates the STOA with multi-period optimal power flow analysis within a master-slave framework to efficiently solve the studied problem. Section 4 provides a detailed description of the test cases, focusing on the analyzed 33- and 69-bus systems, including a parameterization of the objective functions, the network topology, and the operational constraints. Section 5 presents the computational results obtained, as well as a validation of the proposed methodology and comparative analyses against literature-reported results. Finally, Section 6 summarizes the key findings and highlights potential avenues for future research.

2. General MINLP formulation

Below is the mathematical model for the optimal placement and sizing of PVs and D-STATCOMs in electrical distribution networks. This unified representation combines the objective function, the constraints, and the auxiliary equations into a comprehensive framework for addressing the MINLP problem [8].

2.1. Objective Function

The goal of the optimization model is to minimize the total costs, which include energy purchasing, investment, and maintenance expenses. This objective function is represented as follows [7]:

$$\min z_{\text{cost}} = z_1 + z_2, \tag{1}$$

where:

$$z_1 = C_{kWh} T f_a f_c \sum_{h\in\mathcal{H}} \sum_{i\in\mathcal{N}} p_{i,h}^{cg} \Delta h, \tag{2}$$

$$z_2 = C_{pv} f_a \sum_{i\in\mathcal{N}} p_i^{pv} + T \sum_{h\in\mathcal{H}} \sum_{i\in\mathcal{N}} C_{O\&M}^{pv} p_{i,h}^{pv} \Delta h + \gamma \sum_{i\in\mathcal{N}} \left(\omega_1 ({q_i}^{comp})^2 + \omega_2 {q_i}^{comp} + \omega_3\right) {q_i}^{comp}. \tag{3}$$

2.2. Constraints

The constraints ensure system feasibility and operational reliability. These are categorized as follows:

2.2.1. Power flow equations:

$$p_{i,h}^{cg} + p_{i,h}^{pv} - P_{i,h}^{d} = v_{i,h} \sum_{j\in\mathcal{N}} Y_{ij} v_{j,h} \cos(\theta_{i,h} - \theta_{j,h} - \varphi_{ij}), \tag{4}$$

$$q_{i,h}^{cg} + q_{i,h}^{comp} - Q_{i,h}^{d} = v_{i,h} \sum_{j\in\mathcal{N}} Y_{ij} v_{j,h} \sin(\theta_{i,h} - \theta_{j,h} - \varphi_{ij}). \tag{5}$$

2.2.2. Power generation bounds:

$$P_i^{cg,\min} \leq p_{i,h}^{cg} \leq P_i^{cg,\max}, \tag{6}$$

$$Q_i^{cg,\min} \leq q_{i,h}^{cg} \leq Q_i^{cg,\max}, \tag{7}$$

$$x_i^{pv} P_{i,h}^{pv,\min} \leq p_i^{pv} \leq x_i^{pv} P_{i,h}^{pv,\max}, \tag{8}$$

$$p_{i,h}^{pv} = G_{i,h}^{pv} p_i^{pv}. \tag{9}$$

2.2.3. Voltage regulation:

$$v^{\min} \leq v_{i,h} \leq v^{\max}. \tag{10}$$

2.2.4. Device installation constraints:

$$\sum_{i\in\mathcal{N}} x_i^{pv} \leq N_{pv}^{ava}, \tag{11}$$

$$x_i^{comp} Q_i^{comp,\min} \leq q_i^{comp} \leq x_i^{comp} Q_{i,h}^{comp,\max}, \tag{12}$$

$$q_{i,h}^{comp} = q_i^{comp}, \tag{13}$$

$$\sum_{i\in\mathcal{N}} x_i^{comp} \leq N_{comp}^{ava}. \tag{14}$$

2.2.5. Annualization and energy costs:

$$f_a = \frac{t_a}{1-(1+t_a)^{-N_t}}, \tag{15}$$

$$f_c = \sum_{t\in\mathcal{T}} \left(\frac{1+t_e}{1+t_a}\right)^t. \tag{16}$$

2.3. Model characteristics

The unified mathematical model encompasses non-convex, convex, and binary components, reflecting the complexity of the optimization problem. These characteristics are detailed below:

- **Non-convex components:** The Objective Function (1) and the Equality Constraints (4) and (5) exhibit nonlinear and non-convex properties. This behavior primarily arises from the inclusion of trigonometric sine and cosine terms, the interactions between voltage variables, and the cubic expressions.
- **Convex components:** A subset of the model, including the Inequality Constraints (6), (7), and (10), as well as the Equality Constraints (9) and (13), is characterized by a linear and convex behavior. These constraints primarily establish the upper and lower bounds of the decision variables, contributing to the model's overall structure.
- **Binary components:** The binary nature of the model is captured by the Inequalities (8), (11), (12), and (14). These constraints involve discrete decision variables that dictate whether specific actions, such as the installation of PVs or D-STATCOMs, should be implemented in the network.

It is important to note that Equations (15) and (16) are not included in this classification, since they provide constant parameters related to annualization and the projected energy costs over the project's duration.

3. Solution strategy

In this work, the optimization model described by Equations (1)–(14) is addressed using a two-stage methodology. In the master stage, the STOA is employed to determine the optimal placement and sizing of PVs and D-STATCOMs. Once these decision variables have been established, they move on to the follower stage, where a power flow algorithm tailored for distribution networks validates the feasibility of the solution. This stage ensures that the power balance constraints are satisfied while providing a detailed analysis of the voltage profiles and power generation across the network for each scenario. The following sections detail the main components of this solution methodology.

3.1. Slave stage: power flow solution

To evaluate the potential solutions proposed by the master stage (*i.e.*, the STOA), a power flow tool based on the successive approximations method is employed. This tool is integral for solving the nonlinear equality constraints associated with power balance, and it is formulated using a complex variable representation. The primary purpose of the power flow tool is to compute all voltage profiles by iteratively solving the system of equations represented by (4) and (5) while assuming fixed power injection and demand.

The iterative power flow equation, which constitutes the foundation of the successive approximations method, is given in (17) [8]:

$$\mathbb{V}_{d,h}^{t+1} = -\mathbb{Y}_{d,d}^{-1}\left[\text{diag}^{-1}\left(\mathbb{V}_{d,h}^{t,\star}\right)\mathbb{S}_{d,h}^{\star} - \mathbb{Y}_{d,g}\mathbb{V}_{g,h}\right], \tag{17}$$

where:

- $\mathbb{V}_{d,h}^{t+1}$ is the vector containing the voltages at all the demand nodes for the period h during iteration $t+1$.
- $\mathbb{Y}_{d,d}^{-1}$ is the inverse of the sub-matrix of the nodal admittance matrix corresponding to the demand nodes.
- $\mathbb{S}_{d,h}^{\star}$ represents the net complex power at demand nodes, incorporating power injections from DERs and loads:

  $$\mathbb{S}_{d,h}^{\star} = \mathbb{S}_{d,h}^{dg} + \mathbb{S}_{DERs,h}^{b} - \mathbb{S}_{d,h}^{d}.$$

  Here, $\mathbb{S}_{d,h}^{dg}$ refers to conventional DG, $\mathbb{S}_{DERs,h}^{b}$ denotes the power injected by the PVs and D-STATCOMs, and $\mathbb{S}_{d,h}^{d}$ represents the demand.
- $\mathbb{Y}_{d,g}$ is the rectangular sub-matrix of the admittance matrix linking the slack bus to the demand nodes.

- $\mathbb{V}_{g,h}$ is the voltage at the slack bus, which is assumed to be fixed and equal to the nominal substation voltage.

The convergence of the successive approximations method is determined by the stopping criterion defined in Equation (18), where the maximum voltage deviation between iterations is compared against a predefined tolerance ε (set at 1×10^{-10}) [17]:

$$\max_{h} \left| \mathbb{V}_{d,h}^{t+1} - \mathbb{V}_{d,h}^{t} \right| \leq \varepsilon, \quad \forall h \in \mathcal{H}. \tag{18}$$

Once the stopping criterion in Equation (18) has been satisfied, the iterative process is deemed to have converged. At this point, the power injected by the slack bus for each time period h is calculated using Equation (19) [18]:

$$\mathbb{S}_{g,h} = \mathbb{Y}_{d,g}\mathbb{V}_{g,h} + \mathbb{Y}_{g,d}\mathbb{V}_{d,h}, \quad \forall h \in \mathcal{H}, \tag{19}$$

where $\mathbb{S}_{g,h}$ represents the complex power vector injected by the slack bus at time h. This final step ensures that all power flows and voltage profiles are consistent with the proposed solution, validating its feasibility and adherence to system constraints.

3.2. Master stage: the STOA approach

The *sech-tanh optimization algorithm* (*i.e.*, the STOA) is a novel optimization method inspired by mathematical functions, specifically the hyperbolic secant (sech) and the hyperbolic tangent (tanh). This algorithm leverages the unique properties of these functions to effectively explore and exploit the solution space in optimization problems. The STOA belongs to the class of math-inspired metaheuristic techniques, which are designed to address complex continuous optimization challenges by balancing global exploration and local exploitation.

The hyperbolic secant function ($\text{sech}(x) = 2/(e^{x} + e^{-x})$) offers a steep decay towards zero, enabling the focused exploitation of promising regions in the solution space. In contrast, the hyperbolic tangent function ($\tanh(x) = (e^{x} - e^{-x})/(e^{x} + e^{-x})$) exhibits a smooth gradient, facilitating broad exploration throughout the search domain. Figure 1 presents the numerical behavior of both functions around the origin of coordinates. By combining these complementary behaviors, the STOA efficiently identifies optimal or near-optimal solutions, making it particularly well-suited for solving large-scale nonlinear optimization problems.

The STOA's fundamental steps are rooted in the iterative application of hyperbolic transformations to candidate solutions, adjusting their trajectories based on the problem's objective function and constraints. This approach allows the STOA to adapt dynamically to diverse optimization landscapes, thereby ensuring robust application performance.

3.2.1. Problem encoding and initial population The decision variables of our formulation are associated with the optimal placement and sizing of PVs and D-STATCOMs in electrical distribution grids. As an example of the proposed solution encoding, consider a distribution network with 33 nodes, where the optimization problem involves two PV generators and two D-STATCOMs with maximum capacities of 1500 kW and 1200 kvar, respectively. The candidate solution vector is presented below:

$$x_j = \begin{bmatrix} 5 & 18 & 10 & 28 & 876.32 & 1341.50 & 430.20 & 985.40 \end{bmatrix}, \tag{20}$$

The interpretation of this solution vector is as follows:

i. The PV systems are located at buses 5 and 18, with nominal sizes of 876.32 kW and 1341.50 kW, respectively.
ii. The D-STATCOMs are placed at buses 10 and 28, with nominal sizes of 430.20 kvar and 985.40 kvar, respectively.

In this encoding approach, the solution vector x_j corresponds to the j^{th} candidate solution within the population at a given iteration p. The population matrix, denoted as X^{p}, has dimensions $n_s \times n_v$, where n_v is the number of decision variables (*i.e.*, the nodes and sizes of the PVs and D-STATCOMs) and n_s is the total number of candidate

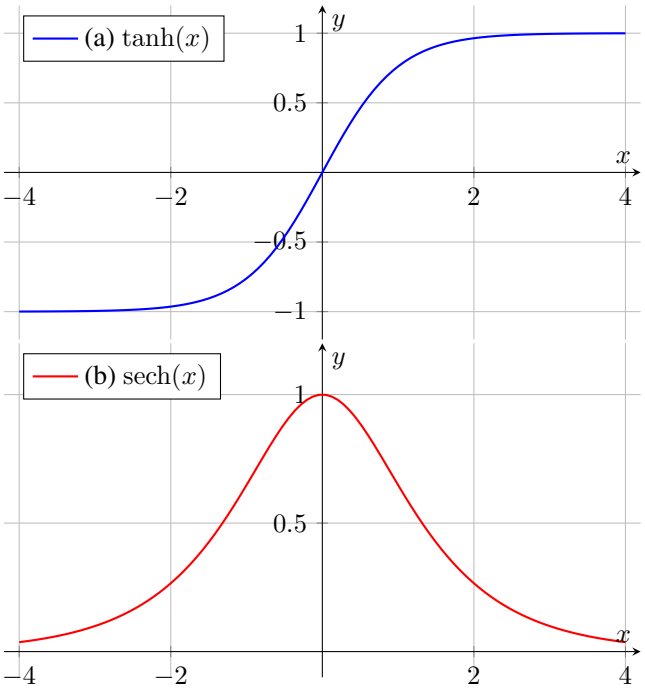

Figure 1. Graphical representation of the $\tanh(x)$ and $\operatorname{sech}(x)$ functions: (a) $\tanh(x)$, and (b) $\operatorname{sech}(x)$

solutions in the population. This encoding ensures that each candidate solution is uniquely defined by its siting and sizing configuration, facilitating the effective exploration and exploitation of the solution space during the optimization process.

To initialize each candidate solution x_j^p for the first iteration ($p = 0$), the values of the decision variables are generated while following the rule specified in Equation (21):

$$x_{j,l} = x_l^{\min} + \beta_l \left(x_l^{\max} - x_l^{\min}\right), \quad \left\{\begin{matrix} l = 1, 2, \ldots, n_v \\ j = 1, 2, \ldots, n_s \end{matrix}\right\}, \tag{21}$$

where:

- β_l is a random variable drawn from a uniform distribution in the range $[0, 1]$, ensuring a stochastic and diverse initialization of decision variables.
- $x_l^{\min}$ and $x_l^{\max}$ represent the lower and upper bounds of the l^{th} decision variable, respectively, defining the feasible search space.

This approach ensures that each decision variable in the candidate solution lies within the predefined limits, promoting an effective exploration of the solution space from the outset of the optimization process. The randomized initialization provided by β_l allows the algorithm to start with a diverse set of solutions, which is critical for achieving global optimization.

3.2.2. Exploration and exploitation rules After initializing the population X^p at iteration $p = 0$, the next step is to identify the best solution within it, denoted as x_{best}^p.

To determine the optimal solution at a given iteration p, all the candidate solutions n_s in the population X^p are evaluated using the objective or fitness function. This process identifies the solution that minimizes the fitness value, as expressed by the following equation:

$$x_{\text{best}}^{p} = \left\{ x_{j}^{p} \mid x_{j}^{p} = \arg\min \left(F_{f}\left(x_{j}^{p}\right) \right),\ \forall j = 1, 2, \ldots, n_{s} \right\}, \tag{22}$$

where x_j^p represents the j^{th} solution in the population at iteration p, and $F_f\left(x_j^p\right)$ is the fitness function value associated with x_j^p.

The fitness function $F_f(x)$ represents the penalized function used to incorporate all inequality constraints in the optimization model – which is generally expressed as $g_k(x) \leq 0,\ k = 1, 2, \ldots, K$ – into the objective function. In the literature, this approach is commonly referred to as the *barrier penalty method*. The proposed fitness function is defined as follows:

$$F_f(x) = z_{\text{cost}} + \sum_{k=1}^{K} \rho_k \max\{g_k(x), 0\}, \tag{23}$$

where ρ_k denotes the penalty factor, which must be carefully tuned in order to balance the objective function value with the constraint violations. It is important to note that the fitness function in (23) is formulated for minimization problems. For maximization problems, the positive sign in the penalty term should be replaced with a negative one.

Once the best solution of the current iteration has been identified, the update rule described in Equation (24) is applied to all candidate solutions $\forall k = 1, 2, \ldots, n_s$:

$$y_{j}^{p} = \begin{cases} x_{j}^{p} + \alpha_1 \cdot \operatorname{sech}(\alpha_2) \cdot \left(\alpha_3 x_{\text{best}}^{p} - (1 - \alpha_3) x_{j}^{p} \right), & \beta \leq \frac{1}{2}, \\ x_{j}^{p} + \alpha_1 \cdot \tanh(\alpha_2) \cdot \left| \alpha_3 x_{\text{best}}^{p} - (1 - \alpha_3) x_{j}^{p} \right|, & \beta > \frac{1}{2}. \end{cases} \tag{24}$$

In this equation, y_j^p represents the candidate solution for the next iteration; α_1 is a linear decay function; α_2 is a vector of random variables uniformly distributed in the range $[-4, 4]$, with dimensions $1 \times n_v$; and α_3 and β are random values uniformly distributed in $[0, 1]$. The parameter α_3 determines the level of influence exerted by the best candidate in the population on the current solution being analyzed. Additionally, the notation $A \cdot B$ indicates the element-wise product of the vectors A and B.

It is worth noting that, for the hyperbolic secant function, the absolute value is not applied, since $0 < \operatorname{sech}(x) \leq 1$. This property enables exploration across the region around x_j^p. In contrast, the hyperbolic tangent function, which is bounded within ± 1, does not require such considerations.

The linear decay function α_1 is updated at each iteration as follows:

$$\alpha_1 = a \left(1 - \frac{p}{p_{\max}} \right), \tag{25}$$

where $p_{\max}$ is the total number of iterations, and a is a user-defined scaling factor. Following the recommendations of [19], a is typically set to a value of 2, *i.e.*, $a = 2$.

Each candidate solution y_k^p is evaluated to ensure it adheres to the predefined bounds of the decision variables. If any variable violates these bounds, it is corrected according to the rule specified in Equation (**??**), which is applied for all $j = 1, 2, \ldots, n_v$ and $l = 1, 2, \ldots, n_s$:

$$y_{j,l}^{p} = \begin{cases} y_{j,l}, & \text{if } x_{l}^{\min} \leq y_{j,l} \leq x_{l}^{\max}, \\ x_{l}^{\min}, & \text{if } y_{j,l} < x_{l}^{\min}, \\ x_{l}^{\max}, & \text{if } y_{j,l} > x_{l}^{\max}. \end{cases} \tag{26}$$

This correction mechanism ensures that any variable exceeding the bounds is adjusted to the nearest permissible value, thereby maintaining the feasibility of the solution.

3.2.3. Population substitution After generating the new candidate solutions, denoted by y_k^p, it is necessary to decide whether they will be included in the population for the next iteration. The performance function value

$F_f\left(y_j^p\right)$ must be evaluated to achieve this. Based on this value, the replacement rule for the population is defined as follows:

$$x_j^{p+1} = \begin{cases} y_j^p, & F_f\left(y_j^p\right) < F_f\left(x_j^p\right) \\ x_j^p, & F_f\left(y_j^p\right) \geq F_f\left(x_j^p\right) \end{cases}, \quad \forall j = 1, 2, ..., n_s. \tag{27}$$

This rule allows updating the population by replacing existing solutions with new candidates if they perform better according to the fitness function.

3.2.4. Stopping criteria In metaheuristic optimization techniques, solutions are iteratively refined through sequential updates. Two common stopping criteria are widely employed in the literature: the optimization process may terminate (i) when the maximum number of iterations specified by the user is reached or (ii) when no improvement in the objective function is observed for $k_{\max}$ consecutive iterations.

For the second criterion, a counter is used to monitor the number of iterations exhibiting no improvement in the objective function value. The parameter $k_{\max}$, which determines the maximum number of non-improving iterations, is defined by the user. It is typically recommended to set $k_{\max}$ as 10-30% of the total number of iterations in order to balance convergence efficiency and exploration.

4. Test feeders and model characterization

This hybrid master-slave optimization strategy, which integrates the STOA with the successive approximations power flow method, was validated on 33- and 69-bus test systems [8]. The electrical layouts of the studied feeders are depicted in Figure 2, while Table 1 outlines their electrical characteristics. These systems have a radial configuration and are designed to operate at a nominal voltage of 12,660 V at the substation level. Additionally, the voltage levels within these feeders are restricted to a permissible range of $\pm 10\%$ [12].

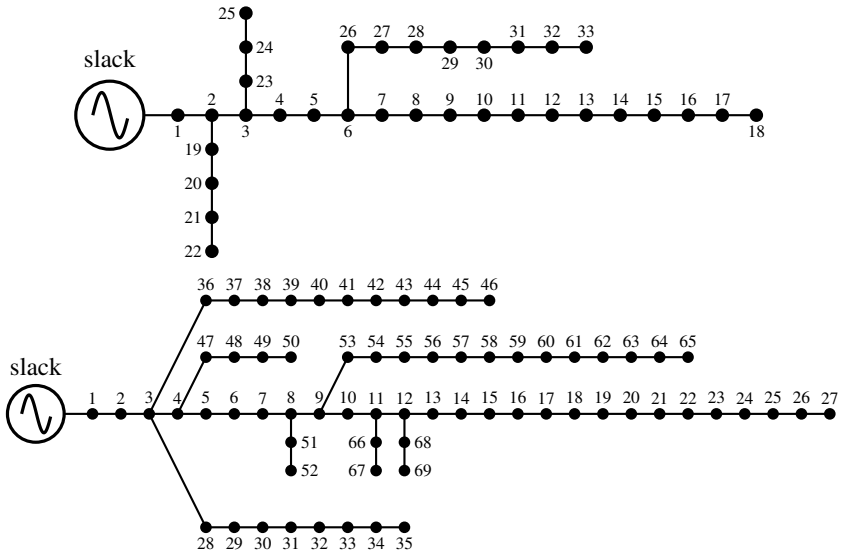

Figure 2. Single-line diagrams of the 33- and 69-bus test feeders

The effectiveness of the proposed method for siting and sizing PVs and D-STATCOMs in medium-voltage distribution networks was evaluated using active and reactive power demand curves (profiles) and average solar power availability data [7]. These curves are illustrated in Figure 3.

Table 1. Branch and load data for the 33- and 69-bus grids

The 33-bus grid											
Node i	**Node j**	**R_{ij} (Ω)**	**X_{ij} (Ω)**	**P_j (kW)**	**Q_j (kvar)**	**Node i**	**Node j**	**R_{ij} (Ω)**	**X_{ij} (Ω)**	**P_j (kW)**	**Q_j (kvar)**
1	2	0.0922	0.0477	100	60	17	18	0.7320	0.5740	90	40
2	3	0.4930	0.2511	90	40	2	19	0.1640	0.1565	90	40
3	4	0.3660	0.1864	120	80	19	20	1.5042	1.3554	90	40
4	5	0.3811	0.1941	60	30	20	21	0.4095	0.4784	90	40
5	6	0.8190	0.7070	60	20	21	22	0.7089	0.9373	90	40
6	7	0.1872	0.6188	200	100	3	23	0.4512	0.3083	90	50
7	8	1.7114	1.2351	200	100	23	24	0.8980	0.7091	420	200
8	9	1.0300	0.7400	60	20	24	25	0.8960	0.7011	420	200
9	10	1.0400	0.7400	60	20	6	26	0.2030	0.1034	60	25
10	11	0.1966	0.0650	45	30	26	27	0.2842	0.1447	60	25
11	12	0.3744	0.1238	60	35	27	28	1.0590	0.9337	60	20
12	13	1.4680	1.1550	60	35	28	29	0.8042	0.7006	120	70
13	14	0.5416	0.7129	120	80	29	30	0.5075	0.2585	200	600
14	15	0.5910	0.5260	60	10	30	31	0.9744	0.9630	150	70
15	16	0.7463	0.5450	60	20	31	32	0.3105	0.3619	210	100
16	17	1.2860	1.7210	60	20	32	33	0.3410	0.5302	60	40
The 69-bus grid											
Node i	**Node j**	**R_{ij} (Ω)**	**X_{ij} (Ω)**	**P_j (kW)**	**Q_j (kvar)**	**Node i**	**Node j**	**R_{ij} (Ω)**	**X_{ij} (Ω)**	**P_j (kW)**	**Q_j (kvar)**
1	2	0.0005	0.0012	0.00	0.00	3	36	0.0044	0.0108	26.00	18.55
2	3	0.0005	0.0012	0.00	0.00	36	37	0.0640	0.1565	26.00	18.55
3	4	0.0015	0.0036	0.00	0.00	37	38	0.1053	0.1230	0.00	0.00
4	5	0.0251	0.0294	0.00	0.00	38	39	0.0304	0.0355	24.00	17.00
5	6	0.3660	0.1864	2.60	2.20	39	40	0.0018	0.0021	24.00	17.00
6	7	0.3810	0.1941	40.40	30.00	40	41	0.7283	0.8509	1.20	1.00
7	8	0.0922	0.0470	75.00	54.00	41	42	0.3100	0.3623	0.00	0.00
8	9	0.0493	0.0251	30.00	22.00	42	43	0.0410	0.0478	6.00	4.30
9	10	0.8190	0.2707	28.00	19.00	43	44	0.0092	0.0116	0.00	0.00
10	11	0.1872	0.0619	145.00	104.00	44	45	0.1089	0.1373	39.22	26.30
11	12	0.7114	0.2351	145.00	104.00	45	46	0.0009	0.0012	29.22	26.30
12	13	1.0300	0.3400	8.00	5.00	4	47	0.0034	0.0084	0.00	0.00
13	14	1.0440	0.3450	8.00	5.50	47	48	0.0851	0.2083	79.00	56.40
14	15	1.0580	0.3496	0.00	0.00	48	49	0.2898	0.7091	384.70	274.50
15	16	0.1966	0.0650	45.50	30.00	49	50	0.0822	0.2011	384.70	274.50
16	17	0.3744	0.1238	60.00	35.00	8	51	0.0928	0.0473	40.50	28.30
17	18	0.0047	0.0016	60.00	35.00	51	52	0.3319	0.1114	3.60	2.70
18	19	0.3276	0.1083	0.00	0.00	9	53	0.1740	0.0886	4.35	3.50
19	20	0.2106	0.0690	1.00	0.60	53	54	0.2030	0.1034	26.40	19.00
20	21	0.3416	0.1129	114.00	81.00	54	55	0.2842	0.1447	24.00	17.20
21	22	0.0140	0.0046	5.00	3.50	55	56	0.2813	0.1433	0.00	0.00
22	23	0.1591	0.0526	0.00	0.00	56	57	1.5900	0.5337	0.00	0.00
23	24	0.3463	0.1145	28.00	20.00	57	58	0.7837	0.2630	0.00	0.00
24	25	0.7488	0.2475	0.00	0.00	58	59	0.3042	0.1006	100.00	72.00
25	26	0.3089	0.1021	14.00	10.00	59	60	0.3861	0.1172	0.00	0.00
26	27	0.1732	0.0572	14.00	10.00	60	61	0.5075	0.2585	1244.00	888.00
3	28	0.0044	0.0108	26.00	18.60	61	62	0.0974	0.0496	32.00	23.00
28	29	0.0640	0.1565	26.00	18.60	62	63	0.1450	0.0738	0.00	0.00
29	30	0.3978	0.1315	0.00	0.00	63	64	0.7105	0.3619	227.00	162.00
30	31	0.0702	0.0232	0.00	0.00	64	65	1.0410	0.5302	59.00	42.00
31	32	0.3510	0.1160	0.00	0.00	11	66	0.2012	0.0611	18.00	13.00
32	33	0.8390	0.2816	14.00	10.00	66	67	0.0470	0.0140	18.00	13.00
33	34	1.7080	0.5646	19.50	14.00	12	68	0.7394	0.2444	28.00	20.00
34	35	1.4740	0.4873	6.00	4.00	68	69	0.0047	0.0016	28.00	20.00

The parameters detailed in Table 2 were applied to evaluate the objective function in the PV generation units. Table 3 provides the cost data for the D-STATCOM devices.

5. Numerical assessment

The proposed master-slave optimization framework was implemented using MATLAB (version 2024a) on a system with an AMD Ryzen 7 3700 processor (2.3 GHz) and 16 GB of RAM, running a 64-bit version of Microsoft Windows 10 Single Language. Custom scripts were specifically developed for the SCA and the successive

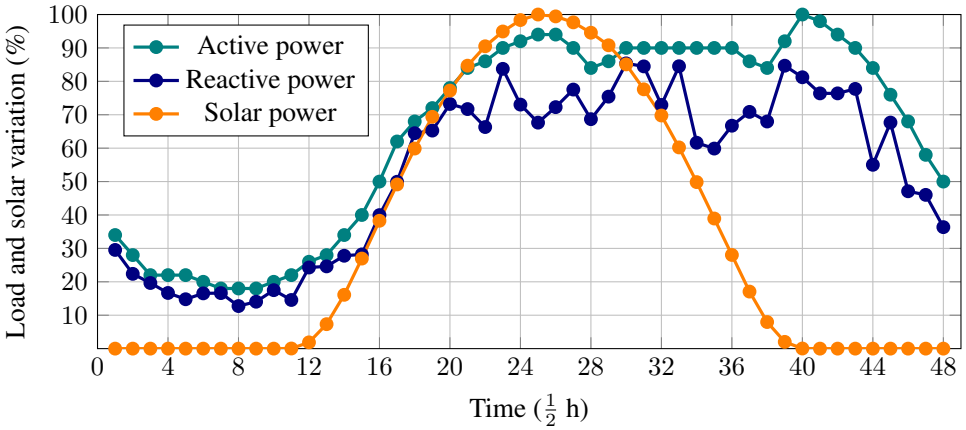

Figure 3. Daily power consumption and solar generation behavior

Table 2. Parameters associated with the optimal location and capacity of PVs in distribution networks

Parameter	Value	Unit	Parameter	Value	Unit
C_{kWh}	0.1390	USD/kWh	T	365	days
t_a	10	%	N_t	20	years
Δh	1	h	t_e	2	%
C_{pv}	1036.49	USD/kWp	C_{0andM}	0.0019	USD/kWh
N_{pv}^{ava}	3	-	$p_i^{pv,\max}$	2400	kW
$P_k^{pv,\min}$	0	kW			

Table 3. Objective function parameters (z)

Par.	Value	Unit	Par.	Value	Unit
ω_1	0.30	USD/Mvar^3	ω_2	-305.10	USD/Mvar^2
ω_3	127,380	USD/Mvar	γ	1/20	—
$Q_i^{comp,\min}$	0	Mvar	$Q_{i,h}^{comp,\max}$	2000	kvar
$P_i^{cg,\min}$	0	W	$P_i^{cg,\max}$	5000	kW
$Q_i^{cg,\min}$	0	var	$Q_i^{cg,\max}$	5000	kvar

approximations power flow method. To assess the performance of the proposed approach, a comparative analysis against the VSA described in [7] was performed. For the experiments, the PV sources were limited to a maximum capacity of 2400 kW, and the D-STATCOMs were capped at 2000 kvar, with a maximum of three PVs and three D-STATCOMs per configuration. All algorithms employed a population size of 50 individuals and were executed over 1000 iterations. Additionally, 100 independent runs were conducted to ensure a robust statistical evaluation of the solution methodologies.

5.1. Results for the 33-bus grid

Table 4 presents comparative analysis of the proposed solution method for the 33-bus grid.

Table 4. Numerical results obtained in the 33-bus grid

Scen.	x_i^{comp} (Node)	q_i^{comp} (Mvar)	x_i^{pv} (Node)	p_i^{pv} (MW)	A_{cost_3} (USD)	Ave. time (s)
Benchmark case	—	—	—	—	3,553,557.38	—
VSA	[6, 15, 31]	[0.3801, 0.0640, 0.3543]	[9, 14, 31]	[0.9844, 0.6312, 1.7602]	2,292,022.62	305.36
SCA	[11, 12, 30]	[0.0092, 0.1143, 0.4617]	[7, 14, 31]	[0.4348, 1.8842, 1.0836]	2,291,234.65	305.97
STOA	[15, 30, 32]	[0.1250, 0.2552, 0.1797]	[12, 16, 32]	[0.8269, 1.0457, 1.5306]	2,290.339.43	314.85

According to the values presented in Table 4, the STOA outperforms both the SCA and the VSA, achieving the lowest project costs for the 33-bus feeder. A detailed analysis of the results is presented below.

i. The STOA achieved the lowest costs, with a total value of $2,290,339.43, which represents a reduction of approximately 35.5480% compared to the benchmark case. This surpasses the reductions achieved by the SCA ($2,291,234.65) and the VSA ($2,292,022.62). The STOA demonstrated a superior ability to minimize costs, resulting in additional savings of $895.22 and $1,683.19 compared to the SCA and the VSA. This makes it the most efficient algorithm for cost optimization in this scenario.
ii. Regarding the placement of PV sources, the STOA identified buses 12, 16, and 32 as the optimal locations, with capacities of 826.9 kW, 1045.7 kW, and 1530.6 kW, respectively. These placements differ from the selections made by the SCA and VSA, but they highlight the potential of these nodes for efficient renewable energy integration. As for the placement of D-STATCOMs, the STOA selected buses 15, 30, and 32, assigning reactive power capacities of 125.0 kvar, 255.2 kvar, and 179.7 kvar. The consistent preference for bus 32 in allocating both PVs and D-STATCOMs underscores its strategic importance in the network.
iii. The STOA also exhibits a competitive computational performance, with an average execution time of 314.85 s. While slightly higher than that of the SCA (305.97 s) and the VSA (305.36 s), this modest increase in computation time is compensated by the substantial cost savings achieved.

The optimal solution obtained by the STOA indicates that approximately 560.0 kvar of reactive power and 3403.2 kWp of active power are required to effectively minimize costs. These values closely align with the ranges reported by the other algorithms, suggesting that the proposed methods converge with similar power requirements while differing in their cost efficiency and resource distribution.

5.2. Results for the 69-bus grid

Table 5 provides a comparative analysis of the numerical results obtained for the 69-bus network.

Table 5. Numerical results obtained in the 69-bus grid

Scen.	x_i^{comp} (Node)	q_i^{comp} (Mvar)	x_i^{pv} (Node)	p_i^{pv} (MW)	A_{cost_3} (USD)	Ave. time (s)
Benchmark case	—	—	—	—	3,723,529.52	—
VSA	[19, 53, 63]	[0.0871, 0.0075, 0.4555]	[15, 33, 62]	[0.8753, 0.5941, 2.0184]	2,400,490.65	1680.10
SCA	[7, 61, 65]	[0.0337, 0.3992, 0.1076]	[18, 59, 61]	[0.8761, 0.3407, 2.2949]	2,396,720.37	1611.16
STOA	[15, 27, 61]	[0.0749, 0.0335, 0.5368]	[26, 61, 64]	[0.2601, 1.9360, 1.3636]	2,394,970.96	2413.23

These numerical results demonstrate the advantages of using the STOA for optimizing the studied 69-bus distribution network. A detailed analysis is presented below.

i. The STOA achieved the lowest costs among the analyzed optimization methods, with a total value of $2,394,970.96. This represents a 35.6801% reduction compared to the benchmark case ($3,723,529.52). The STOA reported savings of $1,029,559.56 compared to the benchmark, $1749.41 compared to the SCA ($2,396,720.37), and $5519.69 compared to the VSA ($2,400,490.65), highlighting its superior capabilities for minimizing costs.
ii. Regarding the placement of PV sources, the STOA selected buses 26, 61, and 64 as the optimal locations, with capacities of 260.1 kW, 1,936.0 kW, and 1,363.6 kW, respectively. These locations imply a more evenly distributed allocation compared to the SCA and VSA, which selected different nodes and exhibited larger variations. The STOA's balanced distribution could contribute to improved grid stability and efficiency.
iii. As for D-STATCOM placement, the STOA selected buses 15, 27, and 61, with reactive power capacities of 74.9 kvar, 33.5 kvar, and 536.8 kvar. This contrasts with the selections made by the SCA and VSA, which targeted different buses and reported lower total reactive power capacities. The STOA's superior reactive power allocation aligns with its cost reduction performance, as it ensures better voltage regulation and reduced losses.
iv. In terms of computational performance, the STOA required an average runtime of 2413.23 s. Although this value is higher in comparison with the SCA (1611.16 s) and the VSA (1680.10 s), the additional

computational effort is justified by the our proposal's ability to achieve the most cost-effective solution. The trade-off between computation time and solution quality is evident, with the STOA delivering superior results regarding cost optimization.

Overall, the STOA demonstrates clear advantages over the SCA and the VSA in terms of cost minimization, balanced resource allocation, and effective PV and D-STATCOM placement. Its ability to reduce costs under feasible and efficient power requirements makes it the most effective optimization method for the 69-bus grid. These findings validate the STOA as a robust and reliable approach for addressing complex optimization challenges in distribution networks.

6. Conclusions and future work

The STOA demonstrated remarkable effectiveness in minimizing costs for both the 33- and 69-bus distribution networks. Compared to the SCA and the VSA, it achieved superior reductions in project costs, highlighting its optimization capabilities. Specifically, in the 33-bus network, our proposal provided additional savings of $895.22 and $1,683.19. Similarly, in the 69-bus network, it surpassed the SCA by $1,749.41 and the VSA by $5,519.69, confirming that it is the most cost-effective optimization method in these scenarios.

The STOA's ability to optimize the placement and sizing of PVs and D-STATCOMs was evident in its solutions. The algorithm consistently identified strategic bus locations and effectively distributed resources to enhance voltage regulation and reduce operating costs. For example, in the 69-bus network, it selected buses 26, 61, and 64 for PV installation and buses 15, 27, and 61 for the D-STATCOMs, demonstrating its proficiency in providing balanced and efficient resource allocation while ensuring network reliability.

Despite requiring slightly longer computation times, the STOA's results compensate for the additional effort with substantial cost reductions and robust solutions. The algorithm's ability to maintain feasibility and scalability across different networks suggests that it is a reliable and adaptable tool for optimizing distribution systems. Its performance highlights its potential for addressing larger and more complex network configurations in future research.

Future research could focus on an expanded comparison of STOA through benchmarking against popular algorithms like PSO, genetic algorithms, and differential evolution to evaluate its performance comprehensively. Additionally, hybrid optimization frameworks that combine the STOA with other techniques could be explored to improve solution quality and computational efficiency. Finally, extending the methodology to multi-objective scenarios and conducting sensitivity analyses would provide insights into its robustness and applicability to real-world challenges in power systems.

ACKNOWLEDGEMENTS

The first author would like to express gratitude to the Research Office of Universidad Distrital Francisco José de Caldas for supporting the internal research project, code 33787724, titled "**Desarrollo de una metodología de gestión eficiente de potencia reactiva en sistemas de distribución de media tensión empleando modelos de programación no lineal**."

REFERENCES

1. Fahad Bin Abdullah, Muhammad Arsalan Aqeeq, Rizwan Iqbal, Maria Abdullah, and Falak Shad Memon. Enhancing electricity distribution efficiency in Pakistan: A framework for progress and action. *Utilities Policy*, 88:101746, June 2024.
2. Mustarum Musaruddin, Tambi Tambi, Waode Zulkaidah, Gamal Abdel Nasser Masikki, Agustinus Lolok, Abdul Djohar, and Marwan Marwan. Optimizing network reconfiguration to reduce power loss and improve the voltage profile in the distribution system: A practical case study. *e-Prime - Advances in Electrical Engineering, Electronics and Energy*, 8:100599, June 2024.
3. Oscar Danilo Montoya, Carlos Alberto Ramírez-Vanegas, and José Rodrigo González-Granada. Dynamic active and reactive power compensation in distribution networks using pv-statcoms: A tutorial using the julia software. *Results in Engineering*, 21:101876, March 2024.

4. Khaled Obaideen, Maryam Nooman AlMallahi, Abdul Hai Alami, Mohamad Ramadan, Mohammad Ali Abdelkareem, Nabila Shehata, and A.G. Olabi. On the contribution of solar energy to sustainable developments goals: Case study on mohammed bin rashid al maktoum solar park. *International Journal of Thermofluids*, 12:100123, November 2021.
5. Sevda Jalali Milani and Gholamreza Nabi Bidhendi. Biogas and photovoltaic solar energy as renewable energy in wastewater treatment plants: A focus on energy recovery and greenhouse gas emission mitigation. *Water Science and Engineering*, 17(3):283–291, September 2024.
6. Ilhan Keskin and Gurkan Soykan. Distribution grid electrical performance and emission analysis of combined cooling, heating and power (cchp)-photovoltaic (pv)-based data center and residential customers. *Journal of Cleaner Production*, 414:137448, August 2023.
7. Adriana Rincón-Miranda, Giselle Viviana Gantiva-Mora, and Oscar Danilo Montoya. Simultaneous integration of d-statcoms and pv sources in distribution networks to reduce annual investment and operating costs. *Computation*, 11(7):145, July 2023.
8. Oscar Danilo Montoya, Walter Gil-González, and Luis Fernando Grisales-Noreña. Optimal planning of photovoltaic and distribution static compensators in medium-voltage networks via the gndo approach. *Results in Engineering*, 23:102764, September 2024.
9. Alejandro Garcés-Ruiz. Power flow in unbalanced three-phase power distribution networks using matlab: Theory, analysis, and quasi-dynamic simulation. *Ingeniería*, 27(3):e19252, August 2022.
10. Abdullah M. Shaheen, Abdullah Alassaf, Ibrahim Alsaleh, and A.M. Elsayed. Enhanced kepler optimization for efficient penetration of pv sources integrated with statcom devices in power distribution systems. *Expert Systems with Applications*, 253:124333, November 2024.
11. Zedequias Machado Alves, Renata Mota Martins, Gustavo Marchesan, and Ghendy Cardoso Junior. Metaheuristic for the allocation and sizing of pv-statcoms for ancillary service provision. *Energies*, 16(1):424, December 2022.
12. Luis Fernando Grisales-Noreña, Daniel Sanin-Villa, and Oscar Danilo Montoya. Optimal integration of pv generators and d-statcoms into the electrical distribution system to reduce the annual investment and operational cost: A multiverse optimization algorithm and matrix power flow approach. *e-Prime - Advances in Electrical Engineering, Electronics and Energy*, 9:100747, September 2024.
13. Farzin Fardinfar and Mostafa Jafari Kermani Pour. Optimal placement of d-statcom and pv solar in distribution system using probabilistic load models. In *2023 10th Iranian Conference on Renewable Energy &; Distributed Generation (ICREDG)*. IEEE, March 2023.
14. Mezigebu Getinet Yenealem. Optimum Allocation of Microgrid and D-STATCOM in Radial Distribution System for Voltage Profile Enhancement Using Particle Swarm Optimization. *International Journal of Photoenergy*, 2024(1), January 2024.
15. Rajiv K. Varma and Ehsan M. Siavashi. Pv-statcom: A new smart inverter for voltage control in distribution systems. *IEEE Transactions on Sustainable Energy*, 9(4):1681–1691, October 2018.
16. Youssef Ait El Kadi, Fatima Zahra Baghli, and Yassine Lakhal. Pv-statcom in photovoltaic systems under variable solar radiation and variable unbalanced nonlinear loads. *International Journal of Electrical and Electronic Engineering &; Telecommunications*, pages 36–48, 2021.
17. Oscar Danilo Montoya, Walter Gil-González, Rubén Iván Bolaños, Diego Fernando Muñoz-Torres, Jesús C. Hernández, and Luis Fernando Grisales-Noreña. Effective power coordination of besus in distribution grids via the sine-cosine algorithm. In *2024 IEEE Green Technologies Conference (GreenTech)*. IEEE, April 2024.
18. Oscar Danilo Montoya and Walter Gil-González. On the numerical analysis based on successive approximations for power flow problems in ac distribution systems. *Electric Power Systems Research*, 187:106454, October 2020.
19. Seyedali Mirjalili. SCA: A Sine Cosine Algorithm for solving optimization problems. *Knowledge-Based Systems*, 96:120–133, March 2016.